ELSEVIER

Biophysical Chemistry 129 (2007) 23–28

Biophysical Chemistry

http://www.elsevier.com/locate/biophyschem

Coupling and internal noise sustain synchronized oscillation in calcium system

Qianshu Li [a,b,*], Ying Wang [a]

[a] The Institute for Chemical Physics, Beijing Institute of Technology, Beijing, 100081, PR China
[b] School of Chemistry and Environment, South China Normal University, Guangzhou, 510006, PR China

Received 9 February 2007; received in revised form 1 May 2007; accepted 1 May 2007
Available online 8 May 2007

Abstract

In this work, the effects of coupling on two calcium subsystems were investigated, the cooperation between coupling and internal noise was also considered. When two non-identical subsystems are in steady state, coupling can induce oscillations, and distinctly enlarge the oscillatory region in bifurcation diagram. Besides, coupling can make the two non-identical oscillators synchronized. With the increment of the coupling strength, the cross-correlation time of the two oscillators firstly increases and then decreases to be constant, showing the synchronization without tuning coupling strength. When internal noise is considered, similar phenomena can also be obtained under the cooperation between coupling and internal noise.

Keywords: Synchronization; Chemical Langevin method; Coupling strength; Internal noise

1. Introduction

A variety of important biological functions are controlled by oscillatory behavior of intracellular calcium [1,2]. The mechanism of an oscillatory Ca^{2+} signal makes cells control and distinguish different Ca^{2+}-regulated intracellular events, and the temporal increase in Ca^{2+} also enables cells to avoid the cytotoxic effects that prolonged increases of the intracellular Ca^{2+} concentration otherwise would exert on cells [3].

It has been shown recently that many types of different signals could be transmitted from cell to cell by oscillation rather than by stationary states in calcium system [4]. Ca^{2+} waves can be propagated in hepatocyte multiplets [5,6], and when stimulated by hormone, coupled hepatocytes can oscillate with the same period, or nearly the same period [7,8]. Such phenomenon of Ca^{2+} entrainment has also been observed in other cell types, such as tracheal ciliated cells [9,10], pancreatic acinar cells [11], and in the blowfly salivary gland [12]. Ca^{2+} signals can spread between cells through two pathways: (a) gap junctions [13–15] and (b) paracrine signaling [16,17]. Individual hepatocytes have very different intrinsic frequencies but become phase-locked when coupled by gap junctions [18]. However, to the best of our knowledge, most of the previous works cared more about wave propagation or synchronization on coupled subsystems when more than one subsystem are in the oscillatory state, so it's necessary to consider the situation when all the coupled subsystems are at quiescence.

The role of internal noise in biological systems has also drawn great interests in recent years: excitability increased by channel noise [19], the emergence of frequency and phase synchronization induced by conductance noise in populations of weakly coupled neurons [20].When internal noise is considered, stochastic calcium oscillations appear in a parameter region where the deterministic model only yields steady state [21]. The influence of internal noise originates from the fluctuations inside the system on coupled calcium subsystems has been investigated [22,23], with one of the subsystems in oscillation state. However, relatively little work has been carried out so far on the influence of internal noise on coupled calcium subsystems when all the subsystems are in steady states.

* Corresponding author. The Institute for Chemical Physics, Beijing Institute of Technology, Beijing, 100081, PR China. Tel./fax: +86 10 6891 2665.
E-mail address: qsli@bit.edu.cn (Q. Li).

0301-4622/$ - see front matter © 2007 Elsevier B.V. All rights reserved.
doi:10.1016/j.bpc.2007.05.001

In the present work, the effects of coupling and internal noise are investigated on two calcium subsystems, with both of them initially lying in the steady state region. Firstly, we coupled two calcium subsystems by using the deterministic model [24], and found that the oscillatory region in bifurcation diagram was enlarged greatly. Furthermore, synchronized oscillations was induced between the two oscillators, and the synchronization without tuning coupling strength occurs. Secondly, the internal noise was taken into account by using Chemical Langevin model. Interestingly, it is shown that the oscillatory region in bifurcation diagram was further increased as a result of the cooperation of internal noise and coupling.

2. Model description

The minimal model discussed in this work, proposed by Dupont et al. [24], is for a gap-junction-dependent mode of intercellular communication. The intercellular communication includes two aspects, the intracellular Ca^{2+} dynamics and the coupling between Ca^{2+} subsystems. A coupled system of the minimal model is considered here and it can be described by the following equations:

$$\begin{aligned}\frac{dz_i}{dt} &= v_0 + v_1\beta_1 - v_2 + v_3 + k_f y_i - kz_i + \gamma(z_j - z_i),\\ \frac{dy_i}{dt} &= v_2 - v_3 - k_f y_i,\end{aligned} \tag{1}$$

where

$$v_2 = V_{M2}\frac{z^n}{K_2^n + z^n}, \quad v_3 = V_{M3}\frac{y^m}{K_R^m + y^m}\cdot\frac{z^p}{K_A^p + z^p}. \tag{2}$$

The index pairs $i, j = 1, 2$ and $2, 1$. γ is the coupling strength and is proportional to the gap junctional permeability. z and y denote the concentration of free Ca^{2+} in the cytosol and in the IP_3-insensitive pool, respectively; v_0 refers to the influx of Ca^{2+} from the extracellular medium; $v_1\beta$ modulates the release of Ca^{2+} from an IP_3-sensitive store into the cytosol. Especially, β measures the saturation of the receptor and is selected as the control parameter, which rises with the level of the stimulus and varies from 0 to 1. More details of the model can be seen in Ref. [24]. The parameter values are: $v_0 = 1\ \mu M\cdot s^{-1}$, $k = 6\ s^{-1}$, $k_f = 1\ s^{-1}$, $v_1 = 7.3\ \mu M\cdot s^{-1}$, $V_{M2} = 65\ \mu M\cdot s^{-1}$, $V_{M3} = 500\ \mu M\cdot s^{-1}$, $K_2 = 1\ \mu M$, $K_R = 2\ \mu M$, $K_A = 0.9\ \mu M$, $m = n = 2$, and $p = 4$.

A deterministic model can only describe the averaged behavior of a system based on large populations. However, due to the finiteness of system size of a cell, the deterministic model cannot account for fluctuations of the behavior in a cell. Stochastic models have been developed based on detailed knowledge of biochemical reactions, molecular numbers, and kinetic rates [25]. Internal noise resulted from the small volume of the system is considered in these stochastic models. The reaction system in this work can be described by a chemical master equation [26], but it's difficult to solve the equation analytically. The chemical Langevin (CL) method [27] has proved to be an efficient simulation algorithm [21,28,29], here the CL equation for the current model reads [21]

Table 1
Stochastic transition processes and corresponding rates [21]

Transition processes	Description	Transition rates
(1) $Z\to Z+1$	A constant input of Ca^{2+} from the extracellular medium to the cytosol	$a_1 = \Omega v_0$
(2) $Z\to Z+1$	Transport of a Ca^{2+} flow from an IP_3-sensitive store (A) into the cytosol	$a_2 = \Omega v_1\beta$
(3) $Z\to Z-1$ $Y\to Y+1$	The pump of Ca^{2+} from the cytosol into the IP_3-sensitive store	$a_3 = \Omega v_2 = \Omega V_{M2} z^n/K_2^n + z^n$
(4) $Z\to Z+1$ $Y\to Y-1$	The release of Ca^{2+} from the IP_3-sensitive store into the cytosol in a process activated by cytosolic Ca^{2+}	$a_4 = \Omega v_3 = \Omega V_{M3} y^m/K_R^m + y^m z^p/K_A^p + z^p$
(5) $Z\to Z+1$ $Y\to Y-1$	Leaky transport of Ca^{2+} from the IP_3-sensitive pool to the cytosol	$a_5 = \Omega k_f y$
(6) $Z\to Z-1$	Transport of cytosolic Ca^{2+} into the extracellular medium	$a_6 = \Omega k z$

$$\begin{aligned}\frac{dz_i}{dt} &= (a_1 + a_2 - a_3 + a_4 + a_5 - a_6) + \frac{1}{\sqrt{\Omega}}\\ &\quad\Big(\sqrt{a_1}\xi_1(t) + \sqrt{a_2}\xi_2(t) - \sqrt{a_3}\xi_3(t) + \sqrt{a_4}\xi_4(t)\\ &\quad + \sqrt{a_5}\xi_5(t) - \sqrt{a_6}\xi_6(t)\Big) + \gamma(z_j - z_i),\\ \frac{dy_i}{dt} &= (a_3 - a_4 - a_5) + \frac{1}{\sqrt{\Omega}}\\ &\quad\Big(\sqrt{a_3}\xi_3(t) - \sqrt{a_4}\xi_4(t) - \sqrt{a_5}\xi_5(t)\Big),\end{aligned} \tag{3}$$

where $\xi_{i=1,\ldots,6}(t)$ are Gaussian white noises with $\langle\xi_i(t)\rangle = 0$ and $\langle\xi_i(t)\xi_j(t')\rangle = \delta_{ij}\delta(t-t')$; Ω is the total cell volume; $z = \frac{Z}{\Omega}, y = \frac{Y}{\Omega}$, Z and Y are the numbers of Ca^{2+} in the cytosol and IP_3-insensitive pool. The additional terms describe internal noise. The meanings of $a_1,\cdots,a_6$ can be seen in Table 1, and the strength of the internal noise terms is scaled as $1/\sqrt{\Omega}$. From the form of CL equation described above, one can easily see that the internal noise is related to the system size. In addition, for identical, symmetrically coupled subsystems, we consider the same level of internal noise.

3. Results and discussion

To probe the influences of coupling and internal noise, it is necessary to investigate the deterministic dynamical behavior of a single system by solving Eq. (1) at $\gamma = 0$. Numerical calculation is performed with the forward Euler method and lasts 5000 s with a time step of 0.001 s. The maximum and minimum values of z are shown in Fig. 1 (dashed lines). With the variation of the control parameter β, the calcium system undergoes two Hopf bifurcation points at $\beta = 0.105$ (left bifurcation point (LBP)) and $\beta = 0.438$ (right bifurcation point (RBP)), respectively. The parameter space is divided into three regions: the low steady state (LSS) region (with lower concentration of calcium), the oscillation state (OS) region, and the high steady state (HSS) region (with higher concentration of calcium).

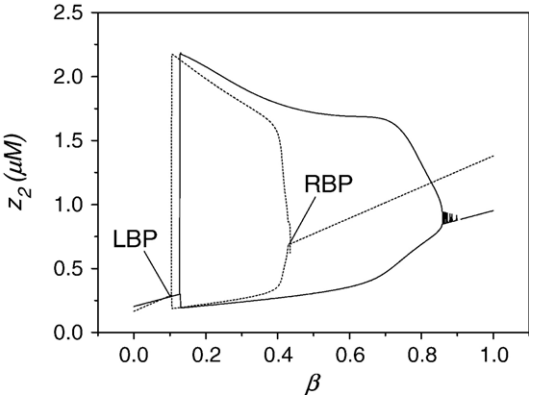

Fig. 1. Schematic bifurcation diagrams for single (dashed lines) and coupled (solid lines) subsystems calculated by deterministic equations. $\beta_{LBP}=0.105$, and $\beta_{RBP}=0.438$ for the single subsystem, and at 0.128 and 0.857 for z_2 at $\beta_1=0.08$ for coupled subsystems.

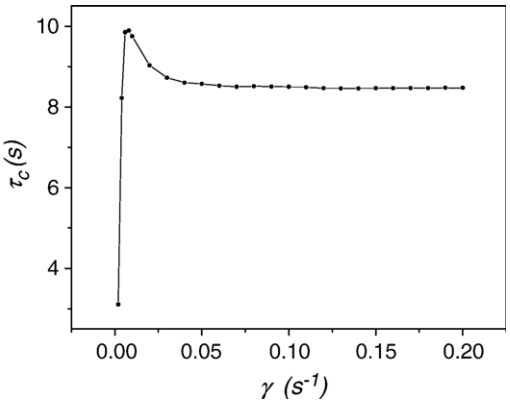

Fig. 3. The cross-correlation time τ_c of the two coupled subsystems *vs.* the coupling strength γ at $\beta_1=0.08$ and $\beta_2=0.5$ in the absence of internal noise.

To probe the effect of coupling on the calcium system, the time series of z_1 and z_2 for $\gamma=0.01$ s^{-1} are plotted in Fig. 2. Fig. 2a shows the results when the parameters β of the two subsystems are tuned in the LSS region ($\beta_1=0.01$, $\beta_2=0.08$). It's obvious that the states of the subsystems cannot dramatically change, and they are still at quiescence. The case is unchanged when both β are tuned in the HSS region (data not shown). However, when β_1 and β_2 are chosen in the LSS region and the HSS region, respectively ($\beta_1=0.5$, $\beta_2=0.05$), oscillation occurs. The time courses of z_1 and z_2 are shown in Fig. 2b. Because the increase in the sum ($v_0+v_1\beta$) brings about the oscillations, which can be triggered by an increase in β due to stimulation by an external signal, or simply by an increase in v_0 originating from an increase in extracellular Ca^{2+} [24]. The underlying mechanism of the oscillations might be that through coupling the Ca^{2+} diffuse between the subsystems and cause the increase of extracellular Ca^{2+}, thus v_0 can be enhanced and result in oscillations. In the last researches, oscillations can be induced by noise or external forces in coupled subsystems, but here coupling can elicit oscillations. In Ref. [30], it is found that in two resting excitable cells when one is stimulated, it can oscillate and drive the other to oscillate, and the oscillations continue after the stimulus terminates. Besides, the oscillations are antiphase, and the pair of cells can be reset to rest by increasing or eliminating the coupling strength. In the present work, coupling draws two resting excitable cells to oscillate. However, the oscillations of both cells are simultaneous and in-phase. In addition, the in-phase oscillations cannot cease with the increment or decrement of the coupling strength. To further explore the effect of coupling, the bifurcation diagram of z_2 is also plotted in Fig. 1 (solid line), with the parameter β_1 fixed at 0.08. The control parameters β_1 is constant, while β_2 is varied, so the values of β_2 in the second oscillator are different from that of β_1 in the first one, assuring that the coupled oscillators are non-identical. It is evident that both bifurcation points shift, LBP shifts a little to the right and the RBP moves to the right greatly. The oscillation range of calcium in a subsystem is much broader than in the isolated system, suggesting that through coupling the oscillation may persist over a much larger parameter range.

In addition, the phenomenon of synchrony can be seen in Fig. 2b. This indicates coupling could induce and sustain synchronized oscillations in two resting cells. In order to quantify the presence of synchrony in the system, the cross-correlation time τ_c is used here to measure the extent of correlation of the two calcium subsystems, and it is calculated for a situation where the

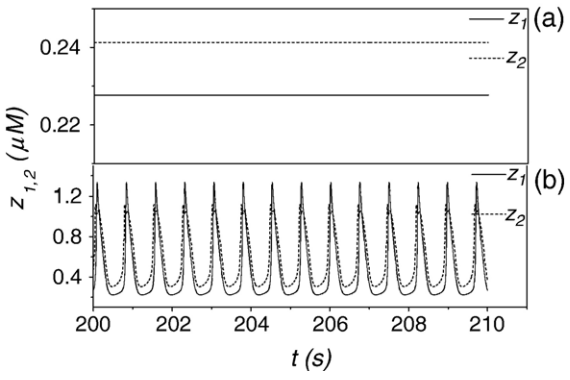

Fig. 2. Time courses of z_1 (solid lines) and z_2 (dashed lines) calculated by deterministic equations at $\gamma=0.01$ (s^{-1}), (a) $\beta_1=0.01$, $\beta_2=0.08$, (b) $\beta_1=0.5$, $\beta_2=0.05$.

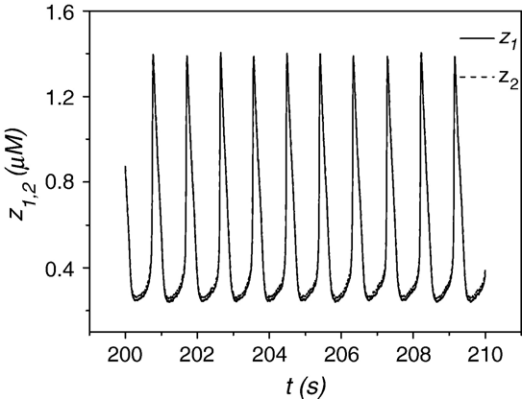

Fig. 4. Time courses of z_1 (solid lines) and z_2 (dashed lines) of the two coupled subsystems calculated by chemical Langevin equations at $\gamma=0.01$ (s^{-1}), $\beta_1=0.5$, and $\beta_2=0.05$.

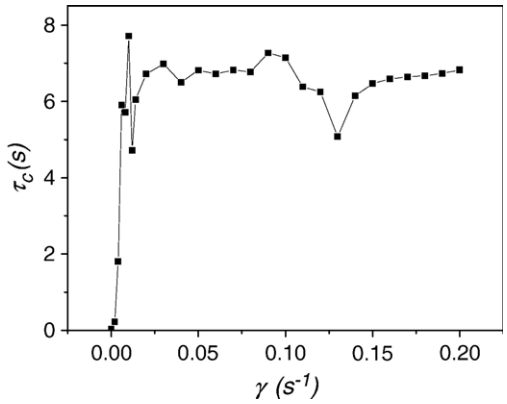

Fig. 5. The cross-correlation time τ_c of the two coupled subsystems *vs*. the coupling strength γ at $\beta_1=0.08$ and $\beta_2=0.5$ in presence of internal noise.

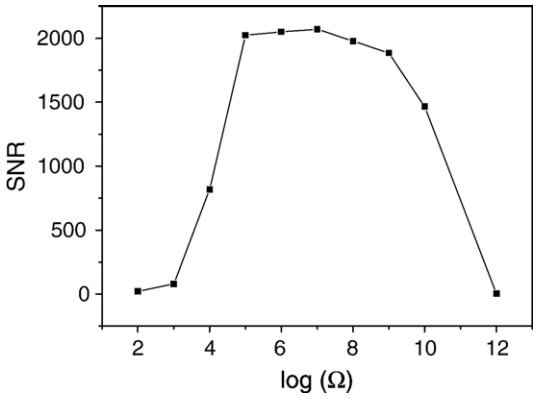

Fig. 7. Dependence of SNR on system size Ω. All data are obtained by averaging twenty independent runs.

isolated systems do not oscillate. The cross-correlation time is defined as [31]

$$\tau_c = \int_0^{+\infty} d\tau \left(\frac{\langle \tilde{y}_1(t)\tilde{y}_2(t+\tau)\rangle}{\langle \tilde{y}_1^2\rangle\langle \tilde{y}_2^2\rangle)^{\frac{1}{2}}} \right)^2, \quad (4)$$

with

$$\tilde{y} = y - \langle y \rangle \quad (5)$$

where $\langle\cdot\rangle$ denotes the average on time. The dependence of τ_c on γ is plotted in Fig. 3. Obviously seeing from Fig. 3, with the increasing of γ, τ_c increases firstly, then decreases slightly and finally reaches a constant. As γ increases to an intermediate value, τ_c approaches a maximum, which implies that the synchronization of the two subsystems shows the best performance. With further increasing γ, τ_c decreases a little but becomes constant above $\gamma=0.01\ s^{-1}$. Because the information is encoded by frequencies between cells, the robustness of τ_c on γ might be in favor of calcium signal propagation.

In nature, the volume of a cell is very small, and the number of reactant molecules in it is small accordingly, so the state of system is discrete and the deterministic equations are no longer applicable. This calls for the use of stochastic methods. Stochastic simulation is done by solving the chemical Langevin equation here. Numerical calculations are performed by using the Eular–Maruyama method with the time step of 0.001 s. Fig. 4 displays time courses of calcium oscillation in the existence of internal noise. From Fig. 4, we can see that the oscillatory frequency decreases compared to Fig. 2 due to the presence of internal noise but the phenomenon of synchronization still exists.

The cross-correlation time τ_c is also used here to measure the synchrony as internal noise is regarded. Compared to Fig. 3, Fig. 5 shows τ_c as a function of the coupling strength γ for $\Omega=10^4\ \mu m^3$. It is manifest that although the cross-correlation time τ_c decreases due to internal noise, and fluctuates, the tendency to approach constant cannot change. That is to say, internal noise would not destroy the synchronization between the two calcium subsystems.

It has been reported that, inside separate cells, internal noise could induce oscillations, and it could even induce coherence resonance in the steady state region close to the bifurcation point [21]. Then, if internal noise is taken into account, will there be oscillation in steady state region where the two subsystems exist? The same parameters as those in Fig. 2 are

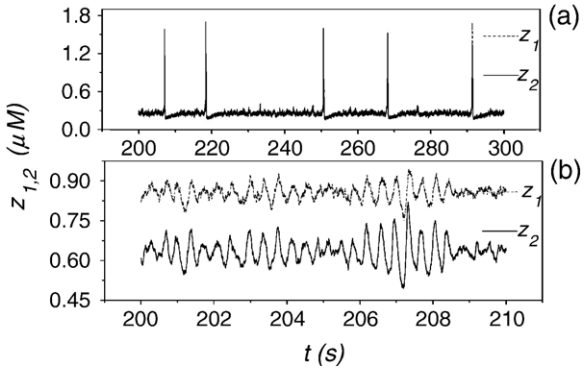

Fig. 6. The dependence of z_1 (dashed lines) and z_2 (solid lines) of the two coupled subsystems on time calculated by chemical Langevin equations at $\gamma=0.01\ (s^{-1})$, and $\Omega=10^4\ \mu m^3$, (a) $\beta_1=0.01$, $\beta_2=0.08$, (b) $\beta_1=0.87$, $\beta_2=0.08$.

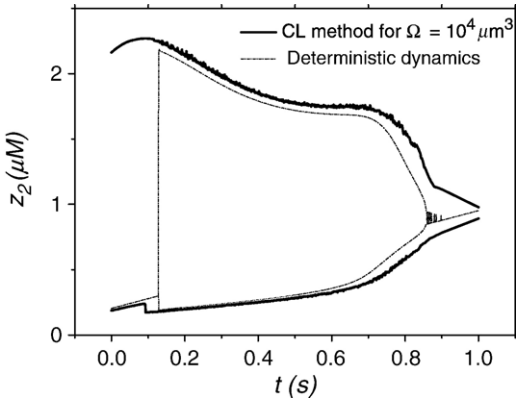

Fig. 8. Schematic bifurcation diagrams for coupled subsystems calculated by deterministic equations (dashed lines). The Hopf bifurcation points occur at $\beta_2=0.128$ and $\beta_2=0.857$ for deterministic equations. The results obtained from chemical Langevin equations are also plotted for a comparison (solid lines).

chosen to plot the time series of calcium concentration in Fig. 6a. Though both β are chosen in the LSS region, spiking behaviors can occur because of internal noise, whereas the phenomenon cannot emerge only through coupling. This points to the effectiveness of internal noise. Besides, as β_1 is fixed at 0.08, the right bifurcation point in Fig. 1 is at $\beta_1 = 0.857$. That means when $\beta_2 > 0.857$, both subsystems are in steady state simultaneously. However, the situation changes as internal noise is under consideration. Fig. 6b shows the time series of calcium concentration at $\beta_1 = 0.87$ and $\beta_2 = 0.08$, one can see oscillation obviously. In the present work, the oscillation cannot appear in a single system in the presence of internal noise or in coupling systems in the absence of internal noise. That is to say, the oscillation is by virtue of the cooperation of internal noise and coupling.

The power spectrum for $\beta_2 = 0.87$ was drawn and there is an obvious peak in it, indicating that there is stochastic oscillation rather than random noise (data not shown). To qualitatively measure the relative performance of the stochastic oscillations, the signal-to-noise ratio (SNR) is defined as in Ref. [32], and the dependence of the SNR on the system size Ω is shown in Fig. 7. The chosen values of Ω cover 10^3 μm^3 which is close to the actual cell volume. There is a peak in the SNR–Ω curve, suggesting there might exist an optimal volume for the coupled subsystems to show the best performance of the stochastic oscillation. When the system size Ω is very large, the stochastic simulations approach the deterministic limit, and the system still stays at the steady state. For very small system size, the internal noise dominates the system, and the oscillation is disordered. For the moderate system size, the system shows stochastic calcium oscillations, and displays strong coherence. This also suggests the occurrence of coherent resonance.

Based on aforementioned discussion, oscillation occurs when internal noise is considered in the region where there is no oscillation originally. The bifurcation diagram of z_2 versus β_2 with β_1 set fixed at 0.08 is presented in Fig. 8, which is plotted to further illuminate the enlargement of oscillation region. One sees that the oscillation region is increased further due to internal noise. That to say, internal noise sustains oscillation further. The mechanism seems to be viewed as the generality in introducing internal noise, because same results have been obtained in Ref. [21,32]. It has been demonstrated that in the cellular regulatory processes, internal noise may enhance the sensitivity of intracellular regulation [33], induce bifurcations which have no counterpart in the deterministic description [34], or facilitate the control of cellular functions [35]. The effectiveness in this work can be seen as another aspect that internal noise benefits biological systems in some cases, and the studies on internal noise in this work might further shed light on the investigation on coupled systems.

4. Conclusions

In conclusion, the effects of coupling in deterministic and mesoscopic dynamics were investigated in calcium subsystems. In the deterministic equations, we found that coupling could induce oscillations in two non-identical subsystems, which were in the steady state region, and enlarge the oscillation region in bifurcation diagram. This implies that coupling benefits synchronized oscillation of the two calcium subsystems when internal noise is absent. Besides, with the increase of coupling strength, the synchronization without tuning the coupling strength occurs. When the mesoscopic equations were studied, the oscillation region in bifurcation diagram could be enlarged further by the cooperation of coupling and internal noise. It might be expected to assess the effectiveness of internal noise on intercellular calcium signaling in living systems, and our findings might be heuristic for information processing in real biological systems.

Acknowledgments

The present work was supported by National Natural Science Foundation of China (Grant No. 20433050), and the 111 Project in China (B07012).

References

[1] M.J. Berridge, P. Lipp, M.D. Bootman, The versatility and universality of calcium signaling, Nat. Rev., Mol. Cell Biol. 1 (2000) 11–21.
[2] M.J. Berridge, The AM and FM of calcium signaling, Nature 386 (1997) 759–760.
[3] C. Oxhamre, A.R. Dahlfors, V.P. Zhdanov, B. Kasemo, A minimal generic model of bacteria-induced intracellular Ca^{2+} oscillations in epithelial cells, Biophys. J. 88 (2005) 2976–2981.
[4] S. Schuster, M. Marhl, T. HÖfer, Modelling of simple and complex calcium oscillations: from single-cell responses to intercellular signalling, Eur. J. Biochem. 269 (2002) 1333–1355.
[5] L. Combettes, D. Tran, T. Tordjmann, M. Laurent, B. Berthon, M. Claret, Ca(2+)-mobilizing hormones induce sequentially ordered Ca2+ signals in multicellular systems of rat hepatocytes, Biochem. J. 304 (1994) 585–594.
[6] S. Patel, L.D. Robb-Gaspers, K.A. Stellato, A.P. Thomas, Coordination of calcium signalling by endothelial-derived nitric oxide in the intact liver, Nat. Cell Biol. 1 (1999) 467–471.
[7] G. Dupont, T. Tordjmann, C. Clair, S. Swillens, M. Claret, L. Combettes, Mechanism of receptor-oriented intercellular calcium wave propagation in hepatocytes, FASEB J. 14 (2000) 279–289.
[8] T. Tordjmann, B. Berthon, M. Claret, L. Combettes, Coordinated intercellular calcium waves induced by noradrenaline in rat hepatocytes: dual control by gap junction permeability and agonist, EMBO J. 16 (1997) 5398–5407.
[9] M.J. Sanderson, A.C. Charles, E.R. Dirksen, Mechanical stimulation and intercellular communication increases intracellular Ca2+ in epithelial cells, Cell Regul. 1 (1990) 585–596.
[10] J. Sneyd, B. Wetton, A. Charles, M.J. Sanderson, Intercellular calcium waves mediated by diffusion of inositol trisphosphate: a two-dimensional model, Am. J. Physiol. 268 (1995) C1537–C1545.
[11] K. Tsaneva-Atanasova, D.I. Yule, J. Sneyd, Calcium oscillations in a triplet of pancreatic acinar cells, Biophys. J. 88 (2005) 1535–1551.
[12] J.A. Rottingen, E. Camerer, I. Mathiesen, H. Prydz, J.G. Iversen, Synchronized Ca2+ oscillations induced in Madin Darby canine kidney cells by bradykinin and thrombin but not by ATP, Cell Calcium 21 (1997) 195–211.
[13] B. Zimmermann, B. Walz, Serotonin-induced intercellular calcium waves in salivary glands of the blowfly *Calliphora erythrocephala*, J. Physiol. 500 (1997) 17–28.
[14] G. Dupont, T. Tordjmann, C. Clair, S. Swillens, M. Claret, L. Combettes, Mechanism of receptor-oriented intercellular calcium wave propagation in hepatocytes, FASEB J. 14 (2000) 279–289.
[15] T. HÖfer, A. Politi, R. Heinrich, Intercellular Ca^{2+} wave propagation through gap-junctional Ca^{2+} diffusion: a theoretical study, Biophys. J. 80 (2001) 75–87.

[16] R. Caroppo, A. Gerbino, L. Debellis, O. Kifor, D.I. Soybel, E.M. Brown, A.M. Hofer, S. Curci, Asymmetrical, agonist-induced fluctuations in local extracellular [Ca(2+)] in intact polarized epithelia, EMBO J. 20 (2001) 6316–6326.
[17] S.F. Schlosser, A.D. Burgstahler, M.H. Nathanson, Isolated rat hepatocytes can signal to other hepatocytes and bile duct cells by release of nucleotides, Proc. Natl. Acad. Sci. U. S. A. 93 (1996) 9948–9953.
[18] T. HÖfer, Model of intercellular calcium oscillations in hepatocytes: synchronization of heterogeneous cells, Biophys. J. 77 (1999) 1244–1256.
[19] J.A. White, J.A. Rubinstein, A.R. Kay, Channel noise in neurons, Trends Neurosci. 23 (2000) 131–137.
[20] J.M. Casado, Synchronization of two Hodgkin–Huxley neurons due to internal noise, Phys. Lett., A 310 (2003) 400–406.
[21] H.Y. Li, Z.H. Hou, H.W. Xin, Internal noise stochastic resonance for intracellular calcium oscillations in a cell system, Phys. Rev., E Stat. Phys. Plasmas Fluids Relat. Interdiscip. Topics 71 (2005) 061916.
[22] M.E. Gracheva, J.D. Gunton, Intercellular communication via intracellular calcium oscillations, J. Theor. Biol. 221 (2003) 513–518.
[23] M.E. Gracheva, R. Toral, J.D. Gunton, Stochastic effects in intercellular calcium spiking in hepatocytes, J. Theor. Biol. 212 (2001) 111–125.
[24] A. Goldbeter, G. Dupont, M.J. Berridge, Minimal model for signal-induced Ca^{2+} oscillations and for their frequency encoding through protein phosphorylation, Proc. Natl. Acad. Sci. U. S. A. 87 (1990) 1461–1465.
[25] T. Tian, K. Burrage, Stochastic models for regulatory networks of the genetic toggle switch, Proc. Natl. Acad. Sci. U. S. A. 103 (2006) 8372–8377.
[26] N.G. Van Kampen, Stochastic Processes in Physics and Chemistry, North-Holland, Amsterdam, 1981.
[27] D.T. Gillespie, The chemical Langevin equation, J. Chem. Phys. 113 (2000) 297–306.
[28] H.Y. Li, Z.H. Hou, H.W. Xin, Internal noise enhanced detection of hormonal signal through intracellular calcium oscillations, Chem. Phys. Lett. 402 (2005) 444–449.
[29] M. Yi, Y. Jia, Q. Liu, J.R. Li, C.L. Zhu, Enhancement of internal-noise coherence resonance by modulation of external noise in a circadian oscillator, Phys. Rev., E Stat. Phys. Plasmas Fluids Relat. Interdiscip. Topics 73 (2006) 041923.
[30] A. Sherman, J. Rinzel, Rhythmogenic effects of weak electrotonic coupling in neuronal models, Proc. Natl. Acad. Sci. U. S. A. 89 (1992) 2471–2474.
[31] A.S. Pikovsky, M. Rosenblum, J. Kurths, Phase synchronization of chaotic oscillators by external driving, Physica, D 104 (1997) 219–238.
[32] Z.H. Hou, H.W. Xin, Internal noise stochastic resonance in a circadian clock system, J. Chem. Phys. 119 (2003) 11508–11512.
[33] J. Paulsson, O.G. Berg, M. Ehrenberg, Stochastic focusing: fluctuation-enhanced sensitivity of intracellular regulation, Proc. Natl. Acad. Sci. U. S. A. 97 (2000) 7148–7153.
[34] T.B. Kepler, T.C. Elston, Stochasticity in transcriptional regulation: origins, consequences, and mathematical representations, Biophys. J. 81 (2001) 3116–3136.
[35] J. Hasty, J. Pradines, M. Dolnik, J.J. Collins, Noise-based switches and amplifier for gene expression, Proc. Natl. Acad. Sci. U. S. A. 97 (2000) 2075–2080.